Steel and Composite Structures, Vol. 7, No. 5 (2007) 355-376
DOI: http://dx.doi.org/10.12989/scs.2007.7.5.355

Viscoelastic behavior on composite beam using nonlinear creep model

Sung-Yeop Jung†

Pyunghwa Institute of Construction Technology,
1474-21, Kwanyang-2-Dong, Dongan-Gu, Anyang City, Kyonggi-Do, 431-810, Korea

Nam-Il Kim‡ and Dong Ku Shin‡†

Department of Civil and Environmental Engineering, Myongji University,
San 38-2, Nam-Dong, Yongin City, Kyonggi-Do, 449-728, Korea

(Received October 13, 2006, Accepted August 31, 2007)

Abstract. The purpose of this study is to predict and investigate the time-dependent creep behavior of composite materials. For this, firstly the evaluation method for the modulus of elasticity of whole fiber and matrix is presented from the limited information on fiber volume fraction using the singular value decomposition method. Then, the effects of fiber volume fraction on modulus of elasticity of GFRP are verified. Also, as a creep model, the nonlinear curve fitting method based on the Marquardt algorithm is proposed. Using the existing Findley's power creep model and the proposed creep model, the effect of fiber volume fraction on the nonlinear creep behavior of composite materials is verified. Then, for the time-dependent analysis of a composite material subjected to uniaxial tension and simple shear loadings, a user-provided subroutine UMAT is developed to run within ABAQUS. Finally, the creep behavior of center loaded beam structure is investigated using the Hermitian beam elements with shear deformation effect and with time-dependent elastic and shear moduli.

Keywords: composite beam; creep; fiber volume fraction; curve fitting method; Marquardt algorithm.

1. Introduction

In fiber-reinforced plastic (FRP) materials, the creep behavior plays an important role in the long-term durability performance of structures or components made of such materials. Creep is a condition in which a material slowly develops deflections due to long-term loads or environmental exposure such as heat effects or changes their material properties due to exposures such as ultra-violet radiation or other environmental factors. Until now, extensive research works have been conducted to evaluate the magnitude of possible time dependent deformations of FRP materials. Because the fiber-reinforced composites are relatively new to the civil engineering field, their long-term durability behavior has not

†Chief Researcher, Corresponding author, E-mail: syjung1@hotmail.com
‡Research Professor
‡†Professor

yet been firmly established. Other complexity of composite materials arises due to possible diversity in designing the composition with combination between fiber and matrix. The mechanical properties of composite materials are greatly influenced by a different fiber volume fraction. In addition, the behavior of composite material can be greatly influenced by temperature change. As the phenomenon of creep is significant, the resulting deformations may need special attention with regard to the long-term structural performance.

It is well known that the fiber volume fraction affects the behavior of FRP materials and intensive research works have been made over the years to investigate its effects. Botelho *et al*. (2003) demonstrated that the tensile and compressive strength increases with the increase of the fiber volume fraction. Qiao *et al*. (2003) studied the effect of fiber volume fraction on flexural-torsional buckling behavior of FRP cantilever I-beam. They showed that the fiber volume fraction is of significant importance for improving the buckling resistance. Bond *et al*. (2002) presented the results of single fiber testing of circular and triangular glass fibers of equivalent cross-section to determine the fiber volume fraction. They used a method in which the removal of the matrix is made by incineration.

On the other hand, the time-dependent effects have been a serious concern for composite structural elements. In the ASCE Structural Plastics Design Manual (SPDM, 1984) for the structural design of plastics and fiber-reinforced composites, a power law model proposed by Findley (1960) was adopted for long-term deformations. It is known that the Findley's power law model is simple to use and provides a reasonable approximation for linear viscoelastic material characterization. Mosallam and Bank (1991) carried out the experimental investigation of time-dependent response of test coupon subjected to uniaxial tension and simple shear with FRP glass/vinyl-ester pultruded sections. There have been creep experiments conducted using a constant stress loading condition. Chambers and Mosallam (1994) reviewed the design basis for creep in composite structures. They verified that the Findley's power law model is an adequate model for representing the first approximation for the time-dependent stress-strain behavior of structural GFRP composites at constant temperature. This approach proved valid for evaluating the time-dependent properties of advanced fiber such as graphite- and Kevlar-epoxy composites for use in construction engineering. McClure and Mohammadi (1995) showed experimental results for compression-creep behavior of thermoset-pultruded GFRP angle sections. The Findley's power law was used successfully to model the creep behavior of the pultruded GFRP angle. Ma *et al*. (1997) investigated the creep properties of carbon fiber reinforced polyetherretherketone (PEEK) $[\pm 45]_{4s}$ laminated composites. Their results on creep strain data showed good agreement with predictions made using the Findley equation. Mottram (1993) used creep test data to determine the long-term behavior and compared it to predictions made using the Findley's linear viscoelastic theory. His study showed that the Findley's creep theory is valid for a wide range of cases and indicated that the pultruded material generally exhibits linear viscoelastic properties. Kesler *et al*. (2003) measured the steady state creep deflection rates of sandwich beams with metallic foam cores and compared the measured results with analytical and numerical predictions of the creep behavior.

Even though a significant amount of research has been conducted for investigation of the fiber volume fraction and the time-dependent effects on the behavior of FRP materials, it is judged that there still remain some margins to improve the study on the viscoelastic behavior of composite materials such as the evaluation method for the modulus of elasticity of fiber and matrix, the reliable creep model, and the calculation of creep deflection. The important points considered in this study are summarized as follows:

1. This study evaluates the modulus of elasticity of fiber and matrix from the limited information on fiber volume fraction using the singular value decomposition method.

2. The existing theoretical and empirical creep models such as the viscoelastic mechanical model and the Findley's power law model are verified.
3. As a creep model, the nonlinear curve fitting method using the iterative procedure based on the Marquardt algorithm (Marquardt, 1963) is proposed.
4. For the time-dependent analysis of a composite material with complex constitutive behavior, a user-supplied material subroutine is developed to run within ABAQUS.
5. Through numerical examples, the creep behavior of beam structure under tension and shear loadings is analyzed. These benchmark tests are considered to represent the behavior of the material in the beam structure and are used to predict the long-term behavior of structures of the same material under the same type of loadings. In addition, the creep behavior of the center loaded beam is investigated using the Hermitian beam elements considering the effect of shear deformation and the time-dependent elastic and shear moduli.

2. Effects of fiber volume fraction and temperature

In order to investigate the constitutive properties of FRP materials, this study utilizes the experimental creep test data published in Plastic Design Library (1991). The material tested is a glass fiber reinforced thermoplastic with polyester PET (Poly Ethylene Terephthalate) resin manufactured by DuPont and the size of specimen is 1.02×0.41×8 cm. For the tests, 30%, 45%, and 55% of glass fiber reinforced materials are used. Product nomenclatures describe the materials as Rynite 530, Rynite 545, and Rynite 555, respectively. Material information such as physical properties, mechanical properties, and thermal properties are presented in Table 1. The creep flexural test produces five data sets, as presented in Table 2.

Table 1 Material properties of GFRP

Fiber Volume Fraction	30%	45%	55%
Physical Properties			
Density (kN/m^3)	15.30	16.57	17.65
Mechanical Properties			
Ultimate tensile strength (GPa)	0.158	0.182	0.196
Elongation at break (%)	2.5	2.0	2.0
Modulus of elasticity (GPa)	10.69	15.51	17.93
Flexural modulus (GPa)	8.96	15.17	17.93
Thermal Properties			
Melting point (℃)	252	252	252

Table 2 Detail of creep flexural test data set

Data set	Fiber volume (%)	Test temperature (℃)
1	30	23
2	45	125
3	45	60
4	45	23
5	55	23

Table 3 Strain data ($\times 10^{-2}$) from creep flexural test with different test conditions

Hours	Data 1	Data 2	Data 3	Data 4	Data 5
1	0.420	0.790	0.410	0.240	0.150
1.7808	0.420	0.800	0.416	0.241	0.150
3.1608	0.421	0.820	0.427	0.241	0.150
31.632	0.429	0.883	0.481	0.260	0.160
100.08	0.450	0.909	0.540	0.264	0.170
237.12	0.460	0.960	0.570	0.272	0.174
316.32	0.470	0.966	0.580	0.276	0.180
562.32	0.480	0.987	0.598	0.290	0.180
1000.8	0.490	1.023	0.630	0.295	0.180
1334.4	0.500	1.050	0.640	0.298	0.180
1778.4	0.510	1.058	0.660	0.303	0.180
2371.2	0.530	1.069	0.670	0.310	0.186
4216.8	0.560	1.103	0.693	0.330	0.203

Table 3 shows the strain data from creep flexural test under different test conditions. From Table 3, it can be found that the GFRP material becomes stiffer as the fiber volume fraction increases under same temperature. On the other hand, the stiffness of GFRP material reduces as the test temperature increases implying possible creep deformations.

3. Evaluation of modulus of elasticity

It is important to determine the effect of fiber volume fraction on the modulus of elasticity for a GFRP. In order to investigate the fiber volume fraction effect on the modulus of elasticity of GFRP, this study proposes a simple but efficient method evaluating the moduli of elasticity of fiber and matrix from the limited fiber volume fraction information. Both of these moduli of elasticity can be extracted from the tabulated information on material properties as shown in Table 1. Experimental creep test data lead to the following set of simultaneous equations for the unknown moduli of elasticity of fiber and matrix.

$$0.3E_f + 0.7E_m = 10.69 \tag{1a}$$

$$0.45E_f + 0.55E_m = 15.51 \tag{1b}$$

$$0.55E_f + 0.45E_m = 17.93 \tag{1c}$$

where E_f and E_m are the modulus of elasticity of fiber and matrix, respectively. Then Eq. (1) can be expressed in matrix form as

$$BX = C \tag{2}$$

where

$$B = \begin{bmatrix} 0.3 & 0.7 \\ 0.45 & 0.55 \\ 0.55 & 0.45 \end{bmatrix} \tag{3a}$$

$$X = \begin{bmatrix} E_f \\ E_m \end{bmatrix} \tag{3b}$$

$$C = \begin{bmatrix} 10.69 \\ 15.51 \\ 17.93 \end{bmatrix} \tag{3c}$$

In this study, to solve Eq. (2), the singular value decomposition (SVD) method is used. The SVD method produces a solution that best approximates in a least-square sense in the case of an overdetermined system (number of data points greater than number of parameters) and underdetermined system (ambiguous combination of parameter exist). From Eq. (2), the matrix can be decomposed into as follows:

$$B = USV^T \tag{4}$$

where U and V are orthogonal matrices, and S is a diagonal matrix. The inverse of Eq. (4) can be expressed as follows:

$$B^{-1} = VS^{-1}U^T \tag{5}$$

The SVD provides a numerically robust solution to the least squares problem. The solution is calculated by the following equation.

$$X = B^{-1}C = B^{-1}(B^T)^{-1}B^TC = (B^TB)^{-1}B^TC = VS^{-1}U^TC \tag{6}$$

After application of the SVD, following result can be obtained.

Table 4 Comparison of given and calculated moduli of elasticity

Fiber volume (%)	Given data (GPa)	Calculated results (GPa)	Percent difference (%)
30	10.69	10.81	1.11
45	15.51	15.19	2.06
55	17.93	18.12	1.05

Table 5 Modulus of elasticity for different fiber volume fraction

Fiber volume (%)	Matrix volume (%)	Modulus of elasticity (GPa)
0	100	2.051
15	85	6.432
30	70	10.814
45	55	15.196
55	45	18.117
70	30	22.499
85	15	26.880
100	0	31.262

$$X = \begin{bmatrix} E_f \\ E_m \end{bmatrix} = \begin{bmatrix} 31.26 \\ 2.05 \end{bmatrix} \tag{7}$$

By substituting Eq. (7) into Eq. (1), the moduli of elasticity for 30%, 45%, and 55% GFRP are calculated to be 10.81, 15.19, and 18.12 GPa, respectively. The comparison of given and calculated elastic moduli is presented in Table 4. It can be seen from Table 4 that the differences between given and calculated elastic moduli are within 2.06%. It is believed that the present SVD method can be applied to calculating the modulus of elasticity of composite material. In Table 5, the calculated values of modulus of elasticity for different fiber volume fraction are also presented.

4. Nonlinear creep models

4.1 Findley's power model

To describe the creep behavior of composite materials, a number of mathematical methods have been proposed in terms of stress, strain, and time. Among these models, the Findley's formulation provides an appropriate approach for describing viscoelastic behavior. The ASCE Structural Plastics Design Manual (1984) presents some rationale for using the Findley's theory. This rationale is as follows: first, it gives fairly simple formulas that describe the creep response of a broad range of plastics including reinforced plastics and laminated plastics. Second, the theory has been verified from experimental tests lasting up to 16 years (Findley and Tracy 1974). The time-dependent viscous strain, resulting from a constant uniaxial tensile stress, can be obtained with the Findley's power creep law as follows:

$$\varepsilon = \varepsilon_o + \varepsilon_t t^n \tag{8}$$

where ε is the total elastic plus time-dependent strain; ε_o is the time-independent initial elastic strain; ε_t is the time-dependent strain, n is the material constant, independent of stress magnitude and t is the elapsed time after loading (in hours).

The Findley's power model contains unknown parameters that can be evaluated from a given creep curve. The empirical material constants can be obtained by using fairly simple curve fitting techniques to match Eq. (8) to experimental strain vs. time curves obtained at several stress levels. Structural Plastic Design Manual (1984) presented the constants in the Findley's creep equation, which were derived from tests of several materials. To obtain the unknown constants in Findley's power law, following equation can be considered from Eq. (8).

$$\log(\varepsilon - \varepsilon_o) = \log\varepsilon_t + n\log(t) \tag{9}$$

At a certain stress level in Eq. (9), a plot of $\log(\varepsilon - \varepsilon_o)$ vs. $\log(t)$ gives a straight line with slope n. Comparing the experimental data and linear regression line, the unknown parameters can be decided.

In the case of pure shear, according to the Findley's power creep law, the strain of an arbitrary point in the laminate can be expressed as:

$$\gamma = \gamma_o + \gamma_t t^n \tag{10}$$

where γ is the total elastic plus time-dependent shear strain; γ_o is the time-independent initial elastic shear strain; γ_t is the time-dependent shear strain. To obtain the shear constants in Findley's power law, a similar equation can be used as with the case of elastic creep strain as shown in Eq. (9).

$$\log(\gamma - \gamma_o) = \log\gamma_t + n\log(t) \tag{11}$$

To predict the long-term creep behavior in the theory of viscoelasticity, the Boltzmann principle of superposition modified by Findley and Khosla (1955) is applied. This principle describes the response of a material by considering different loading histories and is used to estimate the recovery behavior or the effects of superimposing a transient live load upon a sustained dead load. As with assumed linear viscoelastic behavior, this principle shows following characteristics: the response of a material to a given load is independent of the response of the material to any loads. Also, the deformation of a specimen is directly proportional to the applied stress, when all deformations are compared at equivalent times. At a certain time, the response due to change of stress can be added or subtracted on the original behavior at the applied time.

Table 6 show calculated parameters and in Fig. 1, a comparison of data sets between the given creep strain data and the calculated creep strain results by the nonlinear curve fitting method using the Findley's power model is made. It can be found from Fig. 1 that the calculated strain results is in good agreement with published experimental creep data sets and averaged percent differences of strain between them are within 2.5% for all data sets considered.

Table 6 Calculated parameters in Findley's power model

	Data 1	Data 2	Data 3	Data 4	Data 5
n	0.508	0.257	0.256	0.118	0.105
ε_t	0.002	0.046	0.046	0.046	0.030

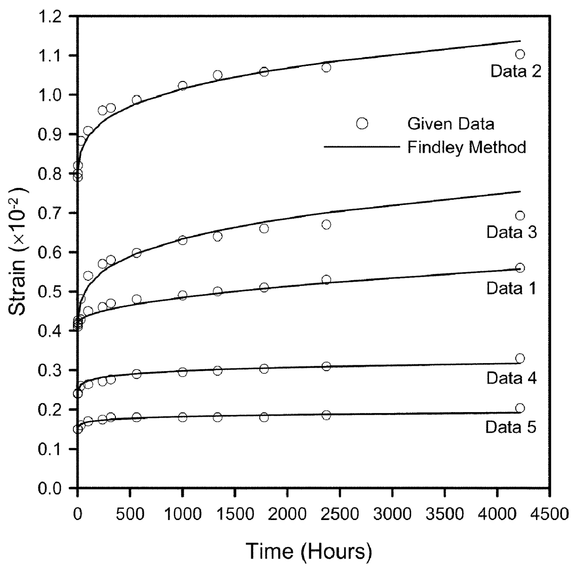

Fig. 1 Comparison of creep strain between given data and evaluated results using Findley's power model

4.2 Creep model based on Marquardt algorithm

As another method to obtain the creep curve from given creep data, this study proposes the nonlinear curve fitting method using the iterative procedure based on the Marquardt algorithm. Recently, Jung (2006) presented the details of the Marquardt algorithm for nonlinear curve fitting techniques. The curve fitting is used to find the "best-fit" curve for a series of data points and it starts with an initial guess for the unknown parameters that are supplied for the subject equation or model. As for a subject equation, this study applies a three-parameter mathematical model proposed by Flugge (1975) consisting of a spring in series with a Kelvin model. The linear viscoelastic behavior by mechanical models can be represented by linear elastic elements, which obey Hook's law, and viscous dashpots, which obey Newton's law of viscosity. The strain response of creep model can be expressed as follows:

$$\varepsilon(t) = \frac{\sigma}{E_1} + \frac{\sigma}{E_2}[1 - \exp(-tE_2/\eta)] \tag{12}$$

where σ is the stress applied to both ends; E_1 and E_2 are the linear spring constants; η is the coefficient of viscosity.

To perform nonlinear curve fitting, Eq. (12) can be modified with a particular choice of parameters.

$$\varepsilon(t) = a_1 + a_2[1 - \exp(-ta_3)] \tag{13}$$

where a_1, a_2 and a_3 are the unknown parameters to be adjusted to achieve a minimum error. After choosing the equation for the model, the chi-square value that represents the sum of the squared error

Table 7 Evaluated parameters in curve fitting method based on Marquardt algorithm

	Data 1	Data 2	Data 3	Data 4	Data 5
a_1	0.4296	0.8211	0.4297	0.2477	0.1507
a_2	0.1298	0.2426	0.2263	6.952E-02	3.421E-02
a_3	6.768E-04	2.918E-03	3.900E-03	1.341E-03	6.304E-03

Table 8 Creep strain results ($\times 10^{-2}$) using the curve fitting method based on Marquardt algorithm

Hours	Data 1	Data 2	Data 3	Data 4	Data 5
1	0.430	0.822	0.431	0.248	0.151
1.7808	0.430	0.822	0.431	0.248	0.151
3.1608	0.430	0.823	0.433	0.248	0.151
31.632	0.432	0.843	0.456	0.251	0.157
100.08	0.438	0.883	0.503	0.256	0.167
237.12	0.449	0.942	0.566	0.267	0.177
316.32	0.455	0.967	0.590	0.272	0.180
562.32	0.471	1.017	0.631	0.285	0.184
1000.8	0.494	1.051	0.651	0.299	0.185
1334.4	0.507	1.059	0.655	0.306	0.185
1778.4	0.521	1.062	0.656	0.311	0.185
2371.2	0.533	1.064	0.656	0.314	0.185
4216.8	0.552	1.064	0.656	0.317	0.185

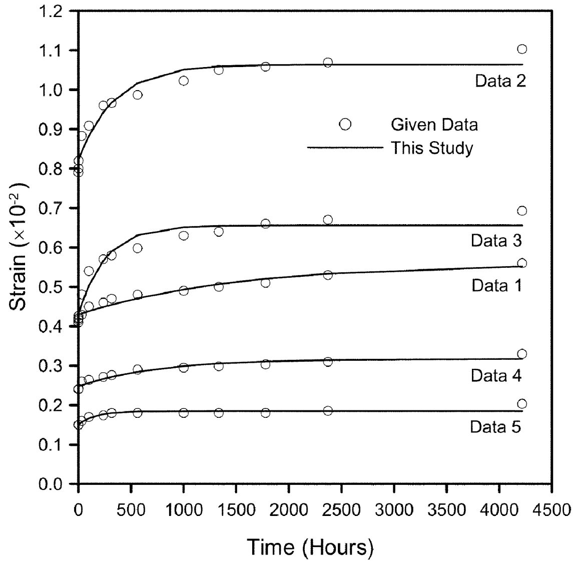

Fig. 2 Creep strain comparison between given data and evaluated results using Marquardt algorithm

between the original data and calculated fit is evaluated. As a nonlinear regression, chi-square regression finds the curve that minimizes the scatter of points around the curve. During the iteration procedure, chi-square is re-evaluated until it finds the best fit. The details of the Marquardt algorithm are presented in Appendix I.

From a nonlinear curve fitting analysis based on the Marquardt algorithm proposed by this study, the calculated parameters in Eq. (13) are presented in Table 7. Also, the strain results using the Marquardt algorithm are presented in Table 8. Fig. 2 depicts the comparison of the given creep strain data and the calculated strain results. It can be found from Fig. 2 that the calculated strain results are in good agreement with the given creep strain data within 3.3% of averaged differences for data set 1 through data set 5.

5. Creep deflection using viscoelastic creep modulus

This study numerically investigates the time-dependent deflection for the simply supported FRP composite beam subjected to lateral force at mid-span. For the short-term behavior of beam, the deflection of a center loaded beam considering shear deformation effect is expressed as (Timoshenko and Gere 1961):

$$\delta = \delta_b + \delta_s = \frac{Pl^3}{48EI} + \frac{f_s Pl}{4GA} \tag{14}$$

where δ is the total deflection; δ_b and δ_s are the deflections due to bending and shear, respectively. P is the applied lateral load at beam center. l is the span length; A is the cross sectional area; I is the moment of inertia; f_s is the shear resistance coefficient. E and G are the elastic and shear moduli, respectively.

On the other hand, the central deflection of beam considering creep behavior for a three point bending of a composite beam can be expressed as:

$$\delta(t) = \delta_b(t) + \delta_s(t) = \frac{Pl^3}{48E(t)I} + \frac{f_s Pl}{4G(t)A} \tag{15}$$

where $\delta(t)$ is the total time-dependent deflection; $\delta_b(t)$ and $\delta_s(t)$ are the time-dependent deflections due to bending and shear, respectively; $E(t)$ and $G(t)$ are the time-dependent elastic and shear moduli, respectively. The $E(t)$ and $G(t)$ can be expressed as follows (Findley *et al.* 1989):

$$E(t) = \frac{E_o E_t}{E_t + E_o t^n} \tag{16a}$$

$$G(t) = \frac{G_o G_t}{G_t + G_o t^n} \tag{16b}$$

where

$$E_o = \frac{\sigma_o}{\varepsilon_o} \tag{17a}$$

$$E_t = \frac{\sigma_t}{\varepsilon_t} \tag{17b}$$

$$G_o = \frac{\tau_o}{\gamma_o} \tag{17c}$$

$$G_t = \frac{\tau_t}{\gamma_t} \tag{17d}$$

For relatively small stresses (or small strains), the power law relationships are converted to a time-dependent elastic modulus, $E(t)$. This modulus is substituted for the conventional modulus, E. In the same manner, time-dependent shear modulus, $G(t)$, can also be obtained.

6. Numerical examples

In this Section, four examples are considered to investigate the influence of fiber volume fraction on creep behavior and to demonstrate the peculiar orthotropic viscoelastic behavior of composite materials. The elastic and shear moduli for the FRP glass/vinyl-ester pultruded sections used in the numerical examples are 16.2 GPa and 3.72 GPa, respectively. These values are the same as the ones given in Mosallam and Bank (1991).

6.1 Nonlinear creep curve estimation for fiber volume fraction

The simulation of the creep strain curve for various fiber volume fractions from given limited data set is carried out. As presented in Table 7, this study uses the parameters in data set 1, 4, and 5 for 30%, 45%, and 55% fiber volume fractions, respectively. With parameters a_1, a_2, and a_3 in Eq. (13), the new parameters a_1', a_2', and a_3' to investigate the effect of various fiber volume fractions are calculated based on the linear least square method. Because the ranges of fiber volume fraction from given creep data are limited, this study simulates creep curves between 30% and 55% of fiber volume fraction. Thus the

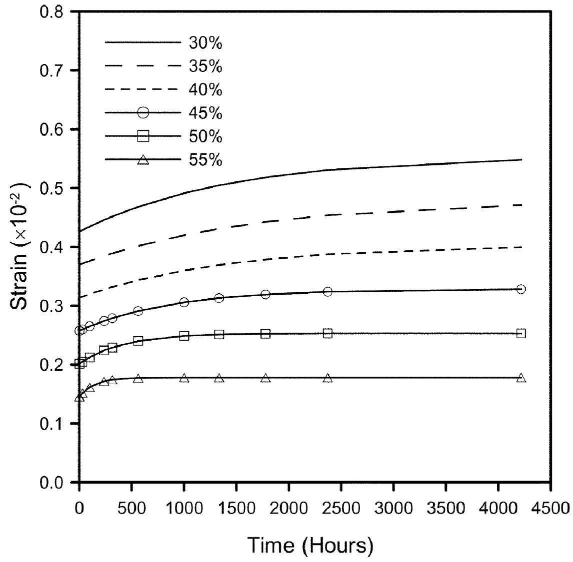

Fig. 3 Estimated creep curve for various combinations of fiber volume fractions

calculated parameters are applied to Eq. (13) and then the creep curves for various combinations of fiber volume fraction are simulated. Estimated creep curves to define the effects of fiber volume fraction are presented in Fig. 3. It can be seen from Fig. 3 that the creep strain decreases and the increasing rate of the creep strain in the primary creep region increases as the fiber volume content increases. In addition, the comparison between the calculated results after simulation in Fig. 3 and the given creep strain data in Table 3 gives the average differences of 1.7%, 3.3%, and 3.5% for fiber volume fraction of 30%, 45%, and 55%, respectively.

6.2 Uniaxial tension creep behavior

In this example, the FRP structure subjected to uniaxial tension with a rectangular cross section that has dimensions of 22.86×1.83×1 cm, as shown in Fig. 4, is considered. The time-dependent analysis of the FRP structure is performed by incorporating the user-provided subroutine UMAT of ABAQUS to reflect the complex constitutive behavior of the constituent material. In the user-supplied subroutine, the material properties are updated for each time step by applying the Findley's power creep model. In the ABAQUS, the C3D8 (8-node linear brick) continuum elements are used and the magnitude of 553.1N per node is applied. For the loaded part of the specimen, the analysis is performed for 2000 hours, while for the unloaded part, the analysis is performed for 200 hours. In order to use the Findley's power creep model, the specific parameters are needed for ε_t and n in Eq. (8). The parameters ε_t and n can be obtained from the test results and are selected as 8.89×10^{-6} and 0.283, respectively.

In Fig. 5, the creep and recovery strains obtained from the present finite element analysis by ABAQUS are presented and compared with the experimental results from Mosallam and Bank (1991). As shown in Fig. 5, the computed strains from ABAQUS agree well with experimental strains.

With the applied load and the creep strain, the creep modulus can be evaluated. Because the creep modulus reflects long-term creep behavior of FRP materials, it is important to establish the value of the creep modulus as follows:

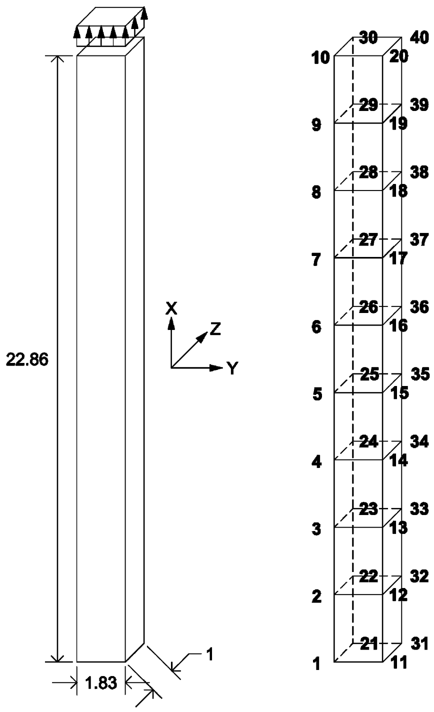

Fig. 4 Dimensions, loading system, coordinate system and node number for uniaxial tension analysis

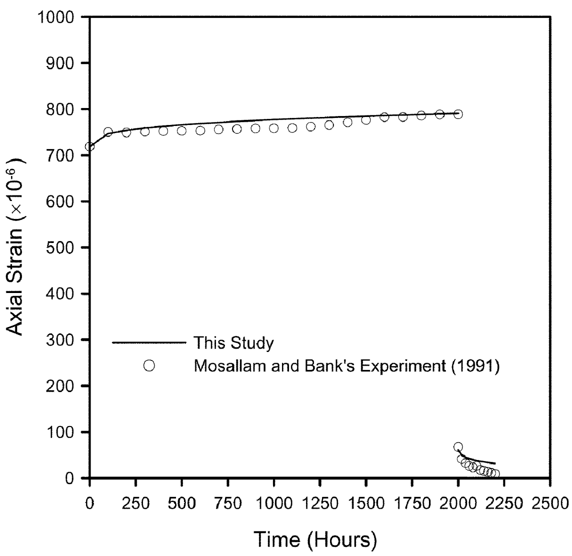

Fig. 5 Comparisons of tensile creep and creep recovery analysis

$$\text{Creep modulus} = \frac{\text{Applied stress}}{\text{Total creep strain}} \tag{18}$$

Fig. 6 shows the evaluated creep modulus versus the time. From Fig. 6, it can be seen that the creep modulus decreases almost linearly with the increase of elapsed time. Using this type of analysis, the

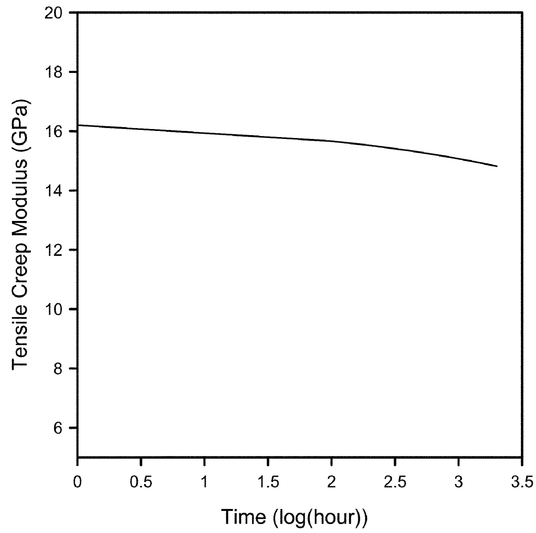

Fig. 6 Tensile creep modulus with respect to the time on a logarithmic scale

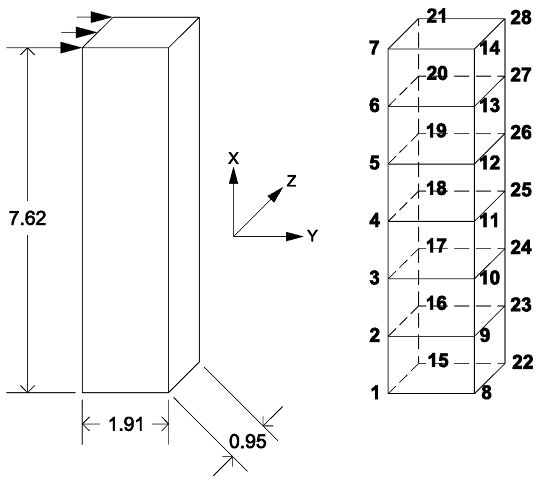

Fig. 7 Dimensions, loading system, coordinate system and node number for simple shear analysis

long-term behavior of composite materials can be extrapolated.

6.3 Simple shear creep behavior

Fig. 7 shows the ABAQUS finite element model which has the dimension of 7.62×1.91×0.95 cm for simple shear creep analysis. Mosallam and Bank (1991) tested the structure in Fig. 7 using an Iosipescu test fixture. In this study, a 200 N shear load is applied directly to the fixture. The Iosipescu test fixture is capable of simulating a simple shear load and one can obtain the in-plane shear properties, such as shear modulus and shear strength, of FRP materials. This test specimen is loaded for 2000 hours and then left unloaded for 90 hours. Under the constant stress shear loading, the shear strain follows the Findley's power law formula. Using the shear test results by Mosallam and Bank (1991), γ_t and n in

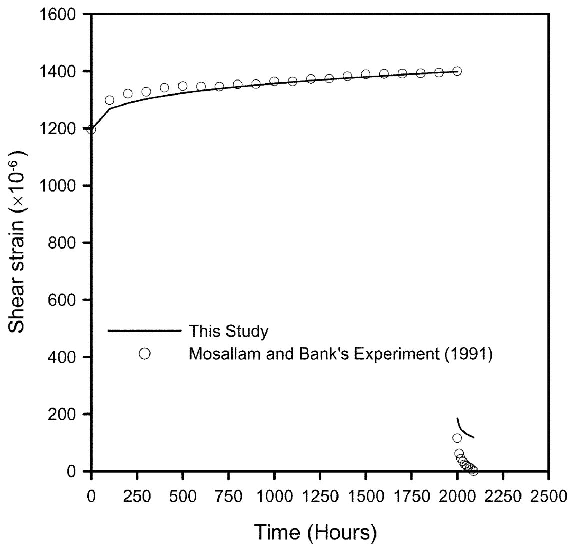

Fig. 8 Comparisons of shear creep and creep recovery analysis

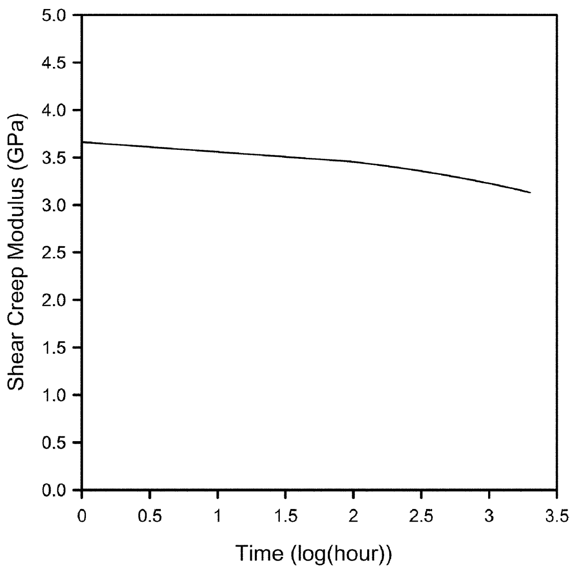

Fig. 9 Shear creep modulus with respect to the time on a logarithmic scale

Eq. (10) are obtained as 22.82×10^{-6} and 0.299, respectively.

Fig. 8 depicts the creep and recovery strains from the finite element analysis and the experimental results from Mosallam and Bank (1991). From Fig. 8, it can be found that the results from this study are in good agreement with the experimental results in the early period of $0 \leq t \leq 2000$ hours for shear creep analysis. While, for shear recovery analysis for $t > 2000$ hours, the results from this study show some differences with experimental results. Although the resulting values shown in Fig. 8 are somewhat different, the trend between them is found to be similar. Additionally, the shear creep modulus over time on a logarithmic coordinate is presented in Fig. 9. This results show very similar trend to the tension test results previously considered in 6.2.

6.4 Creep deflection using viscoelastic creep modulus

In our final example, the time-dependent deflection analysis for the simply supported beam subjected to lateral force at mid-span is performed. Two different beam lengths of 127 cm and 254 cm are considered, while the same wide flange beam section with 20.32×20.32×0.95 cm is used for the beams. The area, moment of inertia and shear coefficient for the beam section are 56.26 cm^2, 4121.52 cm^4, and 3.207, respectively.

To provide an additional verification of the analysis, the finite element formulation considering the shear deformation effect and the time-dependent elastic and shear moduli are presented. To accurately express the element deformation, pertinent shape functions are necessary. For this, the third order Hermitian polynomials are adopted to interpolate the lateral and rotational displacement parameters and the detailed expressions of the interpolation polynomials and the stiffness matrix are presented in Appendix II.

In Tables 9 and 10, the time-dependent deflection at mid-span of FRP beam for 127 cm and 254 cm, respectively obtained from this study using the Hermitian beam elements are presented. For comparison, the analytical solutions derived in Section 5 and the results obtained from the commercial FEM software, ABAQUS are presented. The beam is modeled by using B21 (2-node linear beam) element from ABAQUS element library. From Tables 9 and 10, it can be seen that the analysis results, which is developed by this study show very close agreement with the analytical solutions and with ABAQUS

Table 9 Time-dependent deflection ($\times 10^{-5}$ cm) at mid-span in 3-point loading analysis for FRP beam (l = 127 cm)

Hours	This study	Analytical solutions			ABAQUS
		with shear effect	without shear effect	Error (%)	
0	5.0052	5.0052	2.8425	76.08	5.0229
100	5.2974	5.2974	2.9685	78.45	5.3167
200	5.3631	5.3631	2.9958	79.02	5.3828
300	5.4081	5.4081	3.0145	79.40	5.4280
400	5.4434	5.4434	3.0291	79.70	5.4635
500	5.4729	5.4729	3.0412	79.96	5.4933
600	5.4985	5.4985	3.0517	80.18	5.5189
700	5.5212	5.5212	3.0611	80.37	5.5418
800	5.5418	5.5418	3.0695	80.54	5.5623
900	5.5606	5.5606	3.0772	80.70	5.5814
1000	5.5779	5.5779	3.0842	80.85	5.5989
1100	5.5941	5.5941	3.0908	80.99	5.6152
1200	5.6093	5.6093	3.0970	81.12	5.6304
1300	5.6236	5.6236	3.1029	81.24	5.6446
1400	5.6371	5.6371	3.1084	81.35	5.6584
1500	5.6500	5.6500	3.1136	81.46	5.6713
1600	5.6623	5.6623	3.1186	81.57	5.6838
1700	5.6740	5.6740	3.1234	81.66	5.6954
1800	5.6853	5.6853	3.1280	81.76	5.7069
1900	5.6961	5.6961	3.1324	81.84	5.7178
2000	5.7065	5.7066	3.1366	81.94	5.7282

Table 10 Time-dependent deflection ($\times 10^{-4}$ cm) at mid-span in 3-point loading analysis for FRP beam (l = 254 cm)

Hours	This study	Analytical solutions			ABAQUS
		with shear effect	without shear effect	Error (%)	
0	2.7066	2.7066	2.2740	19.02	2.7206
100	2.8406	2.8406	2.3748	19.61	2.8560
200	2.8701	2.8701	2.3967	19.75	2.8859
300	2.8903	2.8903	2.4116	19.85	2.9063
400	2.9061	2.9061	2.4232	19.93	2.9223
500	2.9193	2.9193	2.4330	19.99	2.9355
600	2.9307	2.9307	2.4414	20.04	2.9472
700	2.9408	2.9409	2.4488	20.10	2.9573
800	2.9501	2.9500	2.4556	20.13	2.9665
900	2.9584	2.9584	2.4617	20.18	2.9751
1000	2.9662	2.9661	2.4674	20.21	2.9827
1100	2.9733	2.9733	2.4727	20.25	2.9901
1200	2.9801	2.9801	2.4776	20.28	2.9969
1300	2.9864	2.9865	2.4823	20.31	3.0033
1400	2.9925	2.9925	2.4867	20.34	3.0094
1500	2.9982	2.9982	2.4909	20.37	3.0152
1600	3.0036	3.0036	2.4949	20.39	3.0208
1700	3.0089	3.0089	2.4987	20.42	3.0259
1800	3.0139	3.0139	2.5024	20.44	3.0310
1900	3.0187	3.0187	2.5059	20.46	3.0358
2000	3.0234	3.0233	2.5093	20.48	3.0406

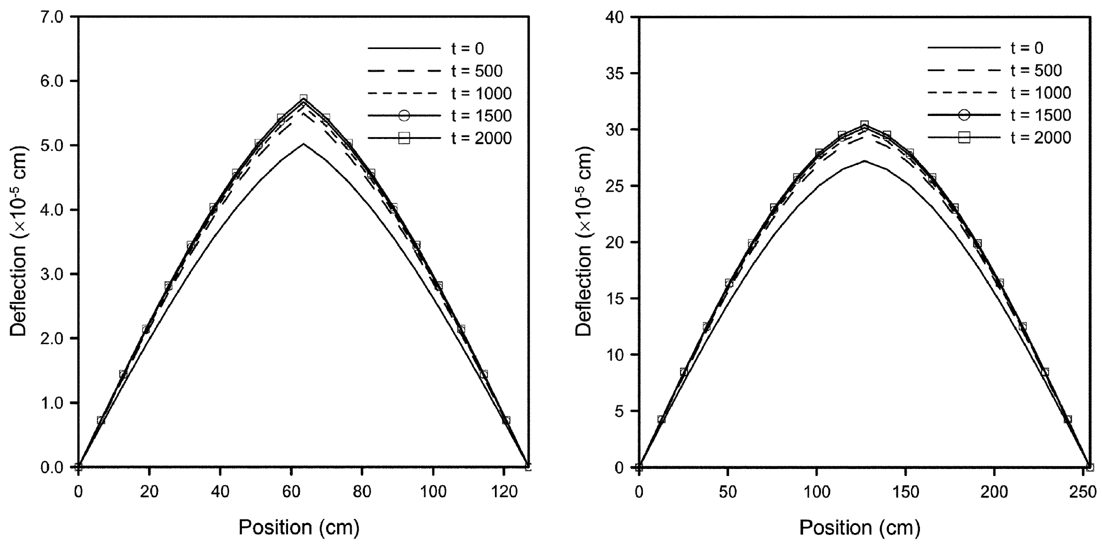

(a) Beam with 127cm length (b) Beam with 254cm length

Fig. 10 Time-dependent deflection with respect to the position for simply supported center loaded FRP beam (l = 127 cm and 254 cm)

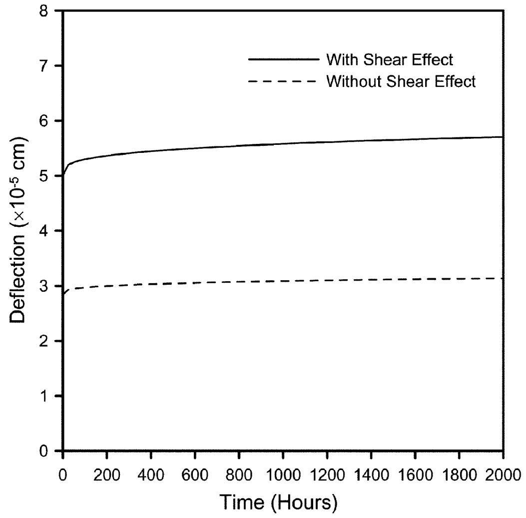

(a) Beam with 127cm length

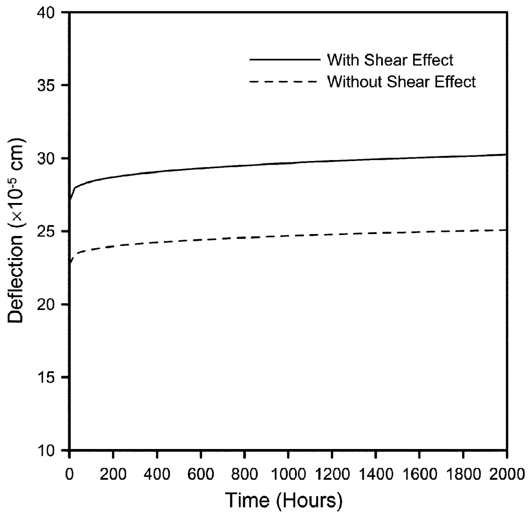

(b) Beam with 254cm length

Fig. 11 Comparisons between with and without shear effects for FRP beam at mid-span deflection (l = 127 cm and 254 cm)

results. Initial maximum deflections of beam are 5.01×10^{-5}cm and 2.71×10^{-4}cm for 127 cm and 254 cm beam length, respectively.

Fig. 10 shows the progress of the time-dependent central deflection of beam for 127 cm and 254 cm length, as time elapses. As shown in Fig. 10(a) for 127 cm FRP beam, the difference of deflection between t = 0, which represent instantaneous deflection and t = 500 hours is found to be 8.55%. The differences of central deflection between t = 500 and t = 1000 hours, t = 1000 and t = 1500 hours, t = 1500 and t = 2000 hours are 1.88%, 1.28%, and 0.99%, respectively. For 254 cm FRP beam, shown in Fig. 10(b), the differences of deflection between t = 0 and t = 500 hours, t = 500 and t = 1000 hours, t = 1000 and t = 1500 hours, t = 1500 and t = 2000 hours are 7.29%, 1.58%, 1.07%, and 0.83%, respectively. Consequently as presented in Fig. 10, the difference of the central deflection becomes smaller as time elapses.

Finally, the effect of shear deformation on the central deflection of beam is presented in Fig. 11. From Fig. 11, significant effect of transverse shear can be seen. The average differences in deflection calculated by including the shear effect is as high as 81.94% and 20.48% for beams with 127 cm and 254 cm, respectively, in comparison with the deflection calculated by ignoring it. As shown in Tables 9

Table 11 Initial deflection at mid-span in 3-point loading analysis for various composite materials

Materials	E_o (GPa)	G_o (GPa)	Length (cm)	with shear effect ($\times10^{-5}$ cm)	without shear effect ($\times10^{-5}$ cm)	Error (%)
Glass/vinyl-ester	16.2	3.72	127	5.005	2.843	76.08
			254	27.07	22.74	19.02
Glass/epoxy	43	4.5	127	2.860	1.071	167.0
			254	12.15	8.569	41.79
Graphite/epoxy	138	7.1	127	1.468	0.334	339.5
			254	4.938	2.670	84.94
Aramid/epoxy	76	2.3	127	4.107	0.606	577.7
			254	11.85	4.848	144.4

and 10 and Fig. 11, the shear effects become more pronounced for the beam with shorter length. Particularly, its effects slightly increase as time elapses. To compare the shear effect of present composite beam with FRP glass/vinyl-ester pultruded sections to that made of other materials, the initial deflections at mid-span for four types of composite materials are presented in Table 11. As can be seen in Table 11, the effect of shear deformation increases as the ratio of E_o/G_o increases.

7. Conclusions

With limited fiber volume fraction test information, this study evaluated the moduli of elasticity of fiber and matrix using the singular value decomposition (SVD) method. Also this study has proposed a nonlinear curve fitting method based on the Marquardt algorithm. Using both representative creep models, this study has verified the effects of fiber volume fraction on the nonlinear creep behavior of composite materials. In addition, to reflect the complex constitutive behavior of the composite material, the creep and recovery analysis of the FRP structures under uniaxial tension and simple shear loads, respectively, was performed by incorporating the user-provided subroutine UMAT of ABAQUS. Finally, the long-term creep behavior of center loaded composite beam was investigated using the Hermitian beam elements with shear deformation effect and time-dependent elastic and shear moduli. Through the numerical examples considered, the following conclusions could be drawn:

1. The elastic moduli calculated from present SVD method are in good agreement with the experimentally measured ones within 2.06% of difference.
2. For the creep and recovery analysis of the FRP structures under uniaxial tension and simple shear loads, the calculated strains by the proposed nonlinear curve fitting method and by the existing Findely's power method agree well with published experimental creep strain data.
3. As the fiber volume content increases, the creep strain decreases and the increasing rate of the creep strain in the primary creep region increases.
4. The uniaxial tension and shear creep moduli are decreased linearly with the increase of elapsed time. Therefore, long-term creep moduli of composite materials can be extrapolated.
5. From the time-dependent deflection analysis of composite beam, the difference in the deflection becomes smaller as time elapses. The shear effects become more pronounced for the beam with shorter length. And its effects slightly increase with increase of elapsed time. Also the effect of shear deformation increases with increase ratio of E_o/G_o.

Acknowledgements

This work is a part of a research project supported by Korea Ministry of Construction & Transportation through Korea Bridge Design & Engineering Research Center at Seoul National University. The authors wish to express their gratitude for the financial support.

References

ABAQUS (2003), *Standard User's Manual, Ver. 6.1*, Hibbit, Karlsson & Sorensen Inc.
ASCE (1984), *Structural Plastics Design Manual*, American Society of Civil Engineering Manuals and Reports

on Engineering Practice.
Asp, E. L., Berglund, A. L. and Talreja, R. (1996), "Prediction of matrix-initiated transverse failure in polymer composites", *Compos. Sci. Tech.*, **56**, 1089-1097.
Bond, I., Hucker, M., Weaver, P., Bleay, S. and Haq, S. (2002), "Mechanical behavior of circular and triangular glass fibers and their composites", *Composites Science and Technology*, **62**, 1051-1061.
Botelho, C. E., Figiel, L., Rezende, C. M. and Lauke, B. (2003), "Mechanical behavior of carbon fiber reinforced polyamide composites", *Compos. Sci. Tech.*, **63**, 1843-1855.
Chambers, E. R. and Mosallam, A. S. (1994), "Design basis for creep composites structures", *Proceedings of the Third Materials Engineering Conference*, San Diego, November.
Findley, N. W. (1960), "Mechanism and mechanics of creep of plastics", *SPE Journal*, January, 57-65.
Findley, N. W. and Khosla, G. (1955), "Application of the superposition principle and theories of mechanical equation of state, strain, and time hardening to creep of plastics under changing loads", *J. Appl. Phy.*, **26**, 821-832.
Findley, N. W., Lai, S. J. and Onaran, K. (1989), *Creep and Relaxation on Nonlinear Viscoelastic Materials*, Dover Publications Inc., New York.
Findley, N. W. and Tracy, F. J. (1974), "16-year creep of polyethylene and PVC", *Polymer Eng. Sci.*, **14**, 577-580.
Flugge, W. (1975), *Viscoelasticity*, *2nd edition*, Springer-Verlag, New York.
Gu, W., Wu, F. H., Kampe, L. S. and Lu, Q. G. (2000), "Volume fraction effects on interfacial adhesion strength of glass-fiber-reinforced polymer composites", *Mater. Sci. Eng.*, **277**, 237-243.
Jung, S. Y. (2006), "Static and viscoelastic investigation of FRP highway bridge deck systems and identification of potential problems", Ph. D. Thesis, University at Buffalo, The State University of New York.
Kesler, O., Crews, K. L. and Gibson J. L. (2003), "Creep of sandwich beams with metallic foam cores", *Mater. Sci. Eng. A*, **341**, 264-272.
Kok, M. M. J. and Meijer, E. H. H. (1999), "Deformation, yield and fracture of unidirectional composites in transverse loading; 1. Influence of fiber volume fraction and test-temperature", *Compos. Part A: Appl. Sci. Manufacturing*, **30**, 905-916.
Liao, K., Schultheisz, R. C. and Hunston, L. D. (1999), "Long-term environmental fatigue of pultruded glass-fiber-reinforced composites under flexural loading", *Int. J. Fatigue*, **21**, 485-495.
Ma, C. C. M., Tai, N. H., Wu, S. H., Lin, S. H., Wu, J. F. and Lin, J. M. (1997), "Creep behavior of carbon-fiber- reinforced polyetherretherketone (PEEK) $[+-45]_{4s}$ laminated composites (I)", *Compos.: Part B*, **28**, 407-417.
Marquardt, W. D. (1963), "An algorithm for least-squares estimation of nonlinear parameters", *J. Society Indus. Appl. Mathematics*, **11**, 431-441.
McClure, G. and Mohammadi, Y. (1995), "Compression creep of pultruded E-glass-reinforced-plastic angles", *J. Mater. Civ. Eng.*, **7**, 269-276.
Mosallam, A. S. and Bank, C. L. (1991), "Creep and recovery of a pultruded FRP frame", *Advanced Composites Materials in Civil Engineering Structures: Proceedings of the specialty conference*, Las Vegas, January.
Mottram, J. T. (1993), "Short- and long term structural properties of pultruded beam assemblies fabricated using adhesive bonding", *Compos. Struct.*, **25**, 387-395.
Plastic Design Library (1991), *The Effect of Creep and Other Time Related Factors on Plastics*, William Andrew, Inc.
Qiao, P., Zou, G. and Davalos, F. J. (2003), "Flexural-torsional buckling of fiber-reinforced plastic composite cantilever I-beams", *Compos. Struct.*, **60**, 205-217.
Timoshenko, P. S. and Gere, M. S. (1961), *Theory of Elastic Stability*, *2nd edition*, McGraw-Hill, New York.
Ye, S. B., Svenson, L. A. and Bank, L. (1995), "Mass and volume fraction properties of pultruded class fiber-reinforced composites", *Composites*, **26**, 725-731.

Appendix I. Nonlinear curve fitting method based on Marquardt algorithm

This study describes a nonlinear curve fitting method when the model depends nonlinearly on the set of M unknown parameters a_k, $k = 1,2,..., M$. The model predicts a functional relationship between the measured independent and dependent variables,

$$\psi(\mu) = \psi(\mu;\ a_1 \dots a_M) = \psi(\mu;a) \tag{A1}$$

To obtain the minimized fitted value for a_k, this study applies the least-square fit using chi-square fit, χ^2. Each data point (μ_i, ψ_i) has its known standard deviation, ξ_i. With chi-square fitting function, the best-fit parameters can be determined by its minimization. The chi-square is the sum of the square of the distances of the points from the curve, divided by the predicted standard deviation.

$$\chi^2(a) = \sum_{i=1}^{N}\left[\frac{\psi_i - \psi(\mu_i;a)}{\xi_i}\right]^2 \tag{A2}$$

The gradient of χ^2 with respect to the parameters a, which will be zero at the χ^2 minimum, has components.

$$\frac{\partial\chi^2}{\partial a_k} = -2\sum_{i=1}^{N}\frac{[\psi_i - \psi(\mu_i;a)]}{\xi_i^2}\frac{\partial\psi(\mu_i;a)}{\partial a_k} \tag{A3}$$

Taking an additional partial derivative for Eq. (A3), following equation can be obtained.

$$\frac{\partial^2\chi^2}{\partial a_k \cdot \partial a_l} = 2 \cdot \sum_{i=1}^{N}\frac{1}{\xi_i^2} \cdot \left[\frac{\partial\psi(\mu_i;a)}{\partial a_k} \cdot \frac{\partial\psi(\mu_i;a)}{\partial a_l} - [\psi_i - \psi(\mu_i;a)] \cdot \frac{\partial^2\psi(\mu_i;a)}{\partial a_l \cdot \partial a_k}\right] \tag{A4}$$

It is conventional to remove the factors of 2 by defining

$$\beta_k \equiv -\frac{1}{2} \cdot \frac{\partial\chi^2}{\partial a_k} \tag{A5a}$$

$$\alpha_k \equiv -\frac{1}{2} \cdot \frac{\partial^2\chi^2}{\partial a_k \cdot \partial a_l} \tag{A5b}$$

Eq. (A5) can be rewritten as the set of linear equations.

$$\sum_{i=1}^{M}\alpha_{kl} \cdot \delta a_l = \beta_k \tag{A6}$$

Eq. (A6) can be solved for the increments δa_l that, added to the current approximation, give the next approximation. Steepest descent method is applied to minimize error for current calculation step.

$$\delta a_l = \text{constant} \times \beta_l \tag{A7}$$

To solve the Eq. (A6) and Eq. (A7), first of all, specific modification is presented for 'constant' in Eq. (A7). In contrast to the quantity, χ^2, has non-dimensional, β_k has the dimensions of $1/\alpha_k$. Also, divide the constant by factor, λ. Then, Eq. (A7) may modify as follows:

$$\delta a_l = \frac{\beta_l}{\lambda \alpha_{ll}} \tag{A8}$$

Second insight in Marquardt method is that Eq. (A6) and Eq. (A8) can be combined if a new matrix, $\tilde{\alpha}$, is defined by the following stipulations.

$$\tilde{\alpha}_{jj} = \alpha_{jj} \ (1+\lambda) \tag{A9a}$$

$$\tilde{\alpha}_{jk} = \alpha_{jk} \ (j \neq k) \tag{A9b}$$

And then, replace both Eq. (A8) and Eq. (A6) by following equation.

$$\sum_{l=1}^{M} \tilde{\alpha}_{kl} \cdot \delta a_l = \beta_k \tag{A10}$$

When λ is very large, the matrix, $\tilde{\alpha}$, is forced into being diagonally dominant, so Eq. (A10) goes over to be identical to Eq. (A8). On the other hand, as λ approaches zero, Eq. (A10) goes over to Eq. (A6). Given an initial guess for the set of fitted parameters a, the Marquardt strategy is as follows:

(1) Compute $\chi^2(a)$.

(2) Pick a modest value for λ, say $\lambda = 0.001$.

(3) Solve the linear equations Eq. (A10) for δa and evaluate $\chi^2(a+\delta a)$.

(4) If $\chi^2(a+\delta a) \geq \chi^2(a)$, increase λ by a factor of 10 and go back to (3).

(5) If $\chi^2(a+\delta a) < \chi^2(a)$, decrease λ by a factor of 10, update the trial solution $a \leftarrow (a+\delta a)$, and go back to (3).

In nonlinear approaches, the minimization must proceed iteratively. Given trial values for the parameters, this study utilizes a procedure that improves the trial solution. The procedure is then repeated until χ^2 stops decreasing by a negligible amount, such as 0.001 as convergence criteria.

Appendix II. Finite element formulation using Hermitian beam elements

The interpolation functions associated with nodal degrees of freedom are assumed to be the linear interpolation polynomial for axial displacement u and the cubic Hermitian polynomials considering shear deformation effect for lateral and rotational displacements which are denoted as v and ω, respectively. As a result, the element displacement parameters can be interpolated with respect to the nodal displacements at p and q as follows:

$$u = (1-\zeta)u^p + \zeta u^q \tag{A11a}$$

$$v = h_1 v^p + h_2 l \omega^p + h_3 v^q + h_4 l \omega^q \tag{A11b}$$

$$\omega = h_5 v^p + h_6 l \omega^p + h_7 v^q + h_8 l \omega^q \tag{A11c}$$

where

$$h_1 = (2\zeta^3 - 3\zeta^2 - 12S\zeta + 1 + 12T)/(1 + 12T) \tag{A12a}$$

$$h_2 = \{\zeta^3 - 2(1 + 3T)\zeta^2 + (1 + 6T)\zeta\}/(1 + 12T) \tag{A12b}$$

$$h_3 = (-2\zeta^3 + 3\zeta^2 + 12T\zeta)/(1 + 12T) \tag{A12c}$$

$$h_4 = \{\zeta^3 - (1 - 6T)\zeta^2 - 6T\zeta\}/(1 + 12T) \tag{A12d}$$

$$h_5 = (6\zeta^2 - 6\zeta)/(1 + 12T) \tag{A12e}$$

$$h_6 = \{3\zeta^2 - 4(1 + 3T)\zeta - 1 + 12T\}/(1 + 12T) \tag{A12f}$$

$$h_7 = (-6\zeta^2 + 6\zeta)/(1 + 12T) \tag{A12g}$$

$$h_8 = \{3\zeta^2 - 2(1-6T)\zeta\}/(1 + 12T) \tag{A12h}$$

$$T = \frac{f_s E(t) I}{G(t) A l^2}, \quad \zeta = \frac{x}{l} \tag{A12j}$$

Substituting the displacement parameters in Eq. (A11a-c) into the elastic strain energy and integrating over the element length, we can obtain the element stiffness matrix in local coordinates as follows:

$$\mathbf{K} = \begin{bmatrix} s_1 & . & . & -s_1 & . & . \\ & s_2 & s_3 & . & -s_2 & s_3 \\ & & s_4 & . & -s_3 & s_5 \\ & & & s_1 & . & . \\ & Symm. & & & s_2 & -s_3 \\ & & & & & s_4 \end{bmatrix} \tag{A13}$$

where

$$s_1 = \frac{E(t)A}{l} \tag{A14a}$$

$$s_2 = \frac{12E(t)I}{(1 + 12T)l^3} \tag{A14b}$$

$$s_3 = \frac{6E(t)I}{(1 + 12T)l^2} \tag{A14c}$$

$$s_4 = \frac{4(1 + 3T)E(t)I}{(1 + 12T)l} \tag{A14d}$$

$$s_5 = \frac{2(1-6T)E(t)I}{(1 + 12T)l} \tag{A14e}$$

CC